Applied Microbiology and Biotechnology (2024) 108:469
https://doi.org/10.1007/s00253-024-13280-6

APPLIED MICROBIAL AND CELL PHYSIOLOGY

Rifaximin ameliorates influenza A virus infection-induced lung barrier damage by regulating gut microbiota

Yijia Zhang[1] · Yafei Chen[1] · Jun Xia[2] · Li Li[1] · Lifeng Chang[1] · Haowei Luo[1] · Jihui Ping[3] · Wenna Qiao[1] · Juan Su[1]

Received: 21 December 2023 / Revised: 5 July 2024 / Accepted: 8 August 2024 / Published online: 19 September 2024

Abstract

Prior research has indicated that the gut-lung-axis can be influenced by the intestinal microbiota, thereby impacting lung immunity. Rifaximin is a broad-spectrum antibacterial drug that can maintain the homeostasis of intestinal microflora. In this study, we established an influenza A virus (IAV)-infected mice model with or without rifaximin supplementation to investigate whether rifaximin could ameliorate lung injury induced by IAV and explore the molecular mechanism involved. Our results showed that IAV caused significant weight loss and disrupted the structure of the lung and intestine. The analysis results of 16S rRNA and metabolomics indicated a notable reduction in the levels of probiotics *Lachnoclostridium*, *Ruminococcaceae_UCG-013*, and tryptophan metabolites in the fecal samples of mice infected with IAV. In contrast, supplementation with 50 mg/kg rifaximin reversed these changes, including promoting the repair of the lung barrier and increasing the abundance of *Muribaculum*, *Papillibacter* and tryptophan-related metabolites content in the feces. Additionally, rifaximin treatment increased ILC3 cell numbers, IL-22 level, and the expression of RORγ and STAT-3 protein in the lung. Furthermore, our findings demonstrated that the administration of rifaximin can mitigate damage to the intestinal barrier while enhancing the expression of AHR, IDO-1, and tight junction proteins in the small intestine. Overall, our results provided that rifaximin alleviated the imbalance in gut microbiota homeostasis induced by IAV infection and promoted the production of tryptophan-related metabolites. Tryptophan functions as a signal to facilitate the activation and movement of ILC3 cells from the intestine to the lung through the AHR/STAT3/IL-22 pathway, thereby aiding in the restoration of the barrier.

Key points

- *Rifaximin ameliorated IAV infection-caused lung barrier injury and induced ILC3 cell activation.*
- *Rifaximin alleviated IAV-induced gut dysbiosis and recovered tryptophan metabolism.*
- *Tryptophan mediates rifaximin-induced ILC3 cell activation via the AHR/STAT3/IL-22 pathway.*

Keywords Rifaximin · Influenza A virus · Tryptophan metabolism · ILC3 cell · Gut-lung axis

Introduction

The influenza virus is composed of four subtypes, namely type A, type B, type C, and type D (Hause et al. 2014). H1N1 is a type of influenza A virus from the *Orthomyxoviridae* family, best known for causing the 2009 global pandemic. The virus has two main surface proteins: hemagglutinin (HA) and neuraminidase (NA), with H1 and N1 being specific subtypes. H1N1 spreads mainly through respiratory droplets from coughs, sneezes, or talking, and can also spread by touching contaminated surfaces and then touching the mouth, nose, or eyes (Liu et al. 2023). At the same time, influenza virus infection also manifests intestinal diseases, such as diarrhea and vomiting. Previous studies have also found that influenza virus-infected animals exhibit disruption of gut microbial

Yijia Zhang and Yafei Chen contributed equally to this work and share first authorship.

✉ Juan Su
sujuan@njau.edu.cn

[1] Laboratory of Animal Neurobiology, College of Veterinary Medicine, Nanjing Agricultural University, Nanjing 210095, China

[2] Institute of Veterinary Medicine, Xinjiang Academy of Animal Science, Urumqi 830013, China

[3] MOE Joint International Research Laboratory of Animal Health and Food Safety, Engineering Laboratory of Animal Immunity of Jiangsu Province, College of Veterinary Medicine, Nanjing Agricultural University, Nanjing 210095, China

community homeostasis (Lu et al. 2019). However, emerging evidence suggests dysbiosis of gut microbes may contribute to lung disease (Zhang et al. 2020). Therefore, microbiota may play an important role in IAV infection. The connection between the microbiota in the digestive system and the respiratory system, which impacts the lung immune system, is referred to as the gut-lung axis (Keely et al. 2012). Inflammation in the lungs can lead to the transfer of inflammatory substances to the intestine via the lung-gut axis, resulting in disturbances in gut microbiota and homeostasis. Conversely, the lungs can also be affected by endotoxins, metabolites, chemokines, or hormones produced by intestinal bacteria through this axis, leading to lung tissue damage (Dumas et al. 2018). Based on the immunological interaction between microbiota and influenza virus, we are exploring interventions in gut microbiota to develop a new strategy for anti-influenza.

As a broad-spectrum antibacterial drug of rifamycin, rifaximin has antibacterial effects on most Gram-positive and some Gram-negative bacteria (Ojetti et al. 2009). Additionally, it has the ability to support the proliferation and growth of beneficial bacteria like *lactic acid bacteria,* aiding in the establishment of a favorable environment for gut probiotics (Luo et al. 2023). Rifaximin has extremely low absorption, is highly safe and effective, and has been proven to effectively improve local and systemic inflammatory responses, reduce the production of bacterial endotoxins and inflammatory cytokines, and maintain mucosal barrier function (DuPont 2016a). Medical clinics frequently utilize it for managing gastroenteropathy, including conditions like inflammatory bowel disease (DuPont 2016b) and irritable bowel syndrome (Gatta and Scarpignato 2017), among others. Therefore, rifaximin, as an important clinical drug for the preventive treatment of intestinal flora imbalance and improving the immune function of the intestinal mucosa, might have great adjuvant therapeutic potential during influenza infection.

The purpose of this study was to create a mouse model of influenza A virus infection with or without the addition of rifaximin in order to examine (a) the impact of influenza A virus infection on lung barrier damage and gut microbial dysbiosis; (b) the effect of rifaximin supplementation in improving lung barrier damage and microbial dysbiosis after exposure to influenza A virus infection; and (c) the mechanisms by which rifaximin mitigates the effects of influenza A virus infection on lung and intestinal barrier dysfunction.

Materials and method

Animals and ethics statement

SPF BALB/c mice, aged 5–6 weeks and of the female gender, were acquired from Xipuerbikai Experimental Animal Company located in Shanghai, China. All animal experiments were conducted under anesthesia. In accordance with the Animal Ethics Procedures and Guidelines of the People's Republic of China and the Institutional Animal Care and Use Committee of Nanjing Agricultural University [SYXK (Su) 2017–0007], the mice were treated with kindness and care. The H1N1 influenza virus used in this experiment was propagated and purified on MDCK cells, and subsequently stored at -80 °C for experimental use. In addition, the titer of the virus is determined by plaque assay.

Mice experiment design

Xipuerbikai Experimental Animal Company in Shanghai provided forty-eight BALB/c mice, all of which were female. The mice were divided into four groups in a random manner, and the treatment details for each group of mice can be found in Table S1. Each group of mice was housed in separate ventilated enclosures and maintained at a consistent temperature (21 ± 1 °C) and humidity (50 ± 10%). The lighting schedule consisted of 14 h of light and 10 h of darkness, with the lights being turned on at 07:00. The day of influenza virus infection was set as day 0. From day 7 before virus infection, the mice were given 50 mg/kg rifaximin with 0.3% CMC turbid liquid or only 0.3% CMC solution via intragastric administration daily until the mice were sacrificed. The mice in the Flu group and Rif + Flu group were given anesthesia using isoflurane on day 0, and then intranasally infected with H1N1 at a dosage equivalent to 2 times the MLD50. The weight of each group of mice was recorded daily until euthanasia. Four days post-infection, six mice from each group were euthanized randomly. Their lung, small intestine, colon tissue, and fecal content were collected for microbial sequencing. At 7 days post-infection, the remaining mice in each group were euthanized, and their collected organs were stored in − 80 °C for western blot and Q-PCR analysis.

Histopathology

After the left lung lobes and colon were recently extracted, they were promptly immersed in a 4% paraformaldehyde solution for 48 h. Subsequently, the tissues were embedded in paraffin and sectioned into 5-μm thick slices. The sections underwent conventional H&E staining to observe pathological alterations and were captured using a microscope with a 400 × objective lens, as previously described (Martinu et al. 2019).

Detection of influenza virus infection by PCR

Total RNA was extracted from the lung and colon homogenates of the mice using Total RNA Extraction Reagent (Vazyme, Nanjing, China) as per the instructions provided

by the manufacturer. Oligo (dT) was used to reverse transcribe two micrograms of total RNA. PCR procedure was performed using primers designed according to the *M* gene of H1N1 virus. The forward primer sequence was 5'—GGA CTGCAGCGTAGACGCTT -3' and the reverse primer sequence was 5'—CATCCTGTTGTATATGAGGCCCAT -3'. The PCR reaction system consisted of 25 μL, including 10 μL of 2 × Taq Master Mix (Dye Plus) from Vazyme in Nanjing, China, 2 μL of both forward and reverse primers, 2 μL of cDNA template, and 9 μL of double-distilled water. The PCR procedure was performed with the following protocol: one round at 95 °C for 5 min, succeeded by 35 rounds at 95 °C for 10 s, 58 °C for 30 s, and 72 °C for 60 s, and one last round at 72 °C for 2 min. PCR products were analyzed by 1.0% agarose gel electrophoresis.

qRT-PCR

Gene expression analysis was conducted using a CFX Connect Real-Time PCR Detection system (Bio-Rad, Berkeley, CA, USA) and AceQ qPCR SYBR Green Master Mix (Vazyme, Nanjing, China), following the manufacturer's guidelines. Primers were synthesized by Generay Biotech (Shanghai, China), and their sequences are listed in Table S2. The levels of gene transcripts were standardized against an internal reference (β-actin).

Western blot analysis

Western blot analysis was performed for protein expression using methods described previously (Chen et al. 2021) with primary antibodies (STAT3, Claudin-1, Occludin, and ZO-1 at dilutions of 1:3000; RORγ, AHR, IDO1 at dilutions of 1:1000; Proteintech). Subsequently, goat anti-mouse IgG-HRP antibody and goat anti-rabbit IgG-HRP secondary antibodies (both at a dilution of 1:1000; Proteintech) were applied. The membranes were incubated with enhanced chemiluminescence (ECL) substrates (Vazyme, Nanjing, China), and signals were detected utilizing an Amersham™ chemiluminescent analyzer (GE Healthcare).

Enzyme-linked immunosorbent assay (ELISA)

The levels of IL-22 protein expression in mouse tissues were assessed using ELISA kits (MMBIO, Jiangsu, China), following the manufacturer's instructions.

Microbial genome DNA extraction

DNA from microbial genomes in mouse stool samples was extracted using HiPure Stool DNA Kits manufactured by Magen in Guangdong, China. The concentration of DNA was measured using a NanoDrop 2000 spectrophotometer. For additional examination, the collected DNA was preserved at a temperature of -20 °C.

Amplification of 16S rRNA genes and sequencing

The V3-V4 regions of the 16S rRNA genes were amplified for microbiota profiling analysis. The forward primer used was 515 F (5'-GTGYCAGCMGCCGCGGTAA-3'), and the reverse primer used was 806R (5'-GGACTACNVGGGTWT CTAAT-3'). Thermal cycling included initial denaturation at 98 °C for 2 min, followed by 30 cycles of denaturation at 98 °C for 10 s, annealing at 55 °C for 30 s, and elongation at 68 °C for 30 s, with a final elongation step at 68 °C for 5 min. PCR products were purified using AMPure XP Beads, quantified with Qubit3.0, and assessed by electrophoresis on a 2% agarose gel. Quantification was confirmed using a Quant-It Pico Green kit and a Qubit Spectrophotometer (Thermo Fisher Scientific). Following a second round of amplification, AMPure XP Beads were used for product purification. Quantification was performed using the ABI OneStepPlus Real-Time PCR System from Life Technologies, USA. Sequencing was conducted using the PE250 mode on a Novaseq 6000 sequencer. Sequencing data were deposited in the NCBI Sequence Read Archive (SRA) under accession numbers from SAMN37928519 to SAMN37928534 in PRJNA1031154.

Targeted organic acid determination

The LC–ESI–MS analysis method was used to determine the critical components of the tryptophan metabolic pathway in the mice fecal samples.

Flow cytometry

The small bowel and respiratory organs were longitudinally sliced into 0.5 cm sections and rinsed in Hanks' Balanced Salt Solution containing 2% FCS. The tissues were then incubated in HBSS with 2 mM EDTA at 37 °C for 20 min in a shaking incubator, and this process was repeated twice. Subsequently, the tissues were digested in complete RPMI with 1 mg / mL Collagenase VIII (Sigma-Aldrich) at 37 °C until complete tissue digestion occurred, approximately 15 min. Peripheral blood underwent red blood cell lysis using lysing buffer (Beyotime, Shanghai, China). Lymphocyte separation was performed using the Percoll lymphocyte separation kit (Solarbio, Beijing, China). Flow cytometric analyses utilized antibodies (Abs) acquired from BD Biosciences. Prior to staining, cells were pre-treated with Mouse BD Fc Block (BD Pharmingen, Franklin Lakes, NJ), then stained with FITC-conjugated anti-CD45 and PE-conjugated anti-RORγt antibodies following the manufacturer's guidelines. Relevant isotype controls were also included. Cell

frequencies were calculated by adding Spherotech Accucount blank particles. Flow cytometry was performed on a FACS Calibur analyzer using FACS Diva 6.2 software (BD Biosciences), and the data were analyzed with FlowJo software.

Statistical analysis

The mean ± standard error of the mean (SEM) was used to present the results for each group. Prior to statistical analysis, we assessed data normality using the Kolmogorov–Smirnov test. Subsequently, one-way ANOVA was performed to analyze significant differences among the four treatment groups using SPSS 25.0 software (SPSS, Chicago, IL, USA).

Results

Establishment of influenza A virus infected and rifaximin treated mice model

We first established the mice model infected with influenza A virus (H1N1) and treated with rifaximin. At 7 days after infection, both the Rif + Flu group (pre-treated with rifaximin and then infected with H1N1) and the Flu group (infected with H1N1 only) showed a significant decrease in body weight compared to the Con group ($p < 0.001$) and the Rif group ($p < 0.001$) (Fig. 1a), indicating that rifaximin can mitigate influenza-induced weight loss. Analysis of average food intake across the four groups of mice (Fig. 1b) revealed variations in food consumption. Notably, food intake consistently decreased in the Flu group and the Rif + Flu group, with rifaximin administration failing to alleviate this reduction.

Influenza virus infection affects not only the lungs but also other organs in the body. We compared the organ indices of the lungs, thymus, and spleen among mice in different treatment groups. Compared to the Con group, the lung index and spleen index showed slight decreases in Fig. S1a-S1b across all three treatment groups, with no notable distinction between the Flu group and the Rif + Flu group. However, the thymus index has no significantly difference between Con, Rif + Flu, Rif and Flu group (Fig. S1c). Similarly, the thymus index did not significantly differ among the Con, Rif + Flu, Rif, and Flu groups (Fig. S1c). These findings suggest that rifaximin had no notable impact on organ weight alterations resulting from influenza infection. Histopathological examination on day 4 post-influenza A virus infection (Fig. 1c) revealed no obvious histological changes in lung and intestine tissues of mice in the Con and Rif groups. However, mice in the

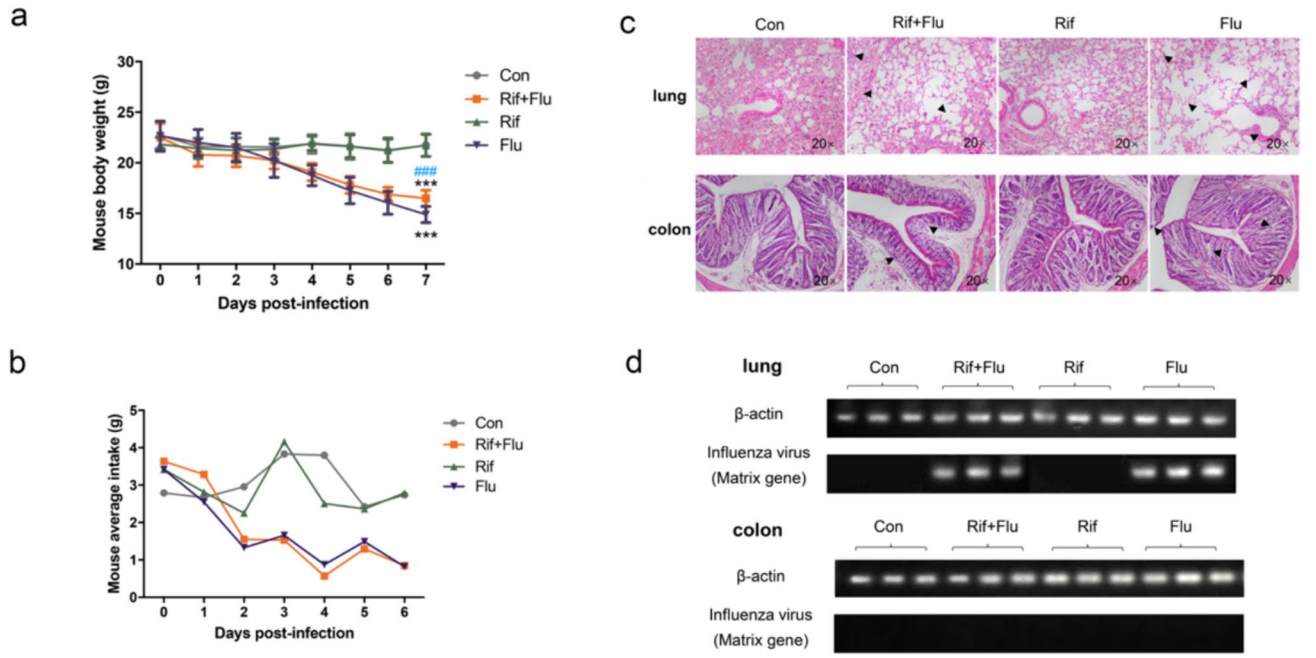

Fig. 1 Rifaximin alleviated the apparent indicators of H1N1 virus infected mice. **a** Body weights of the mice in four groups were measured each day for 7 days following the primary challenge, **b** Changes in average food intake in rifaximin-treated and influenza infected mice, **c** Pathological analysis of the lung and colon sections of the different experimental mice groups. (Light microscopy 200×), **d** Expression of influenza virus M gene in lung and colon tissues at day 7 post-infection. Con: Control group; Rif + Flu: Mice were treated with rifaximin after H1N1 infection.; Rif: Mice treated with rifaximin; Flu: Mice infected with H1N1. *$P < 0.05$; **$P < 0.01$; ***$P < 0.001$; ****$P < 0.0001$. All replicates are biological

Flu group exhibited significant damage characterized by vasodilation, congestion, thickening of the bronchial muscle layer, rupture of the alveolar septum, and infiltration of inflammatory cells. The lung damage in the Rif + Flu group was minimal compared to the Flu group. In the colon tissues, the Con and Rif groups displayed distinct tissue organization without pathological abnormalities. In contrast, the Flu group showed shrinkage of colonic intestinal glands, altered crypt configuration, and detached mucosal epithelial cells. The Rif + Flu group exhibited reduced intestinal gland shrinkage and upward crypt shift. These results demonstrate that influenza A virus not only damages mouse lungs but also affects colon structure. Importantly, rifaximin effectively mitigated influenza-induced lung and colon damage in mice.

RT-PCR results of day 7 post-infection tissue samples from influenza A virus showed efficient replication in the lungs of mice in the Flu group compared to the Rif + Flu group. However, no viral genome was detected in the colon of any group (Fig. 1d). These findings suggest that influenza A virus-induced pathological damage to the colon may not result from direct colonization.

Effect of rifaximin on influenza A virus altered gut microbiota composition

Bacterial diversity Four days after H1N1 influenza A virus infection, we conducted sterile isolation and collected feces from four groups of mice ($n = 4$) to analyze V3-V4 16S rRNA gene profiles. Microbial diversity and richness analysis revealed that the Rif group exhibited a significant decrease in both the Ace index and Shannon index compared to the Con and Flu groups, respectively (Fig. 2 a-d, $p < 0.05$). However, no notable distinction was observed between the Con and Flu groups, suggesting that supplementation with rifaximin significantly enhances the diversity and abundance of microorganisms in mouse feces compared to the Con and Flu groups.

Community membership and structure Next, to assess the similarity of microbial communities in the feces of the four groups of mice, we conducted a β-diversity assay. PCoA analysis, based on weight distance in the fecal samples, revealed distinct separation among the Con, Rif + Flu, Rif, and Flu groups (Fig. 2e-g). Significant differences in

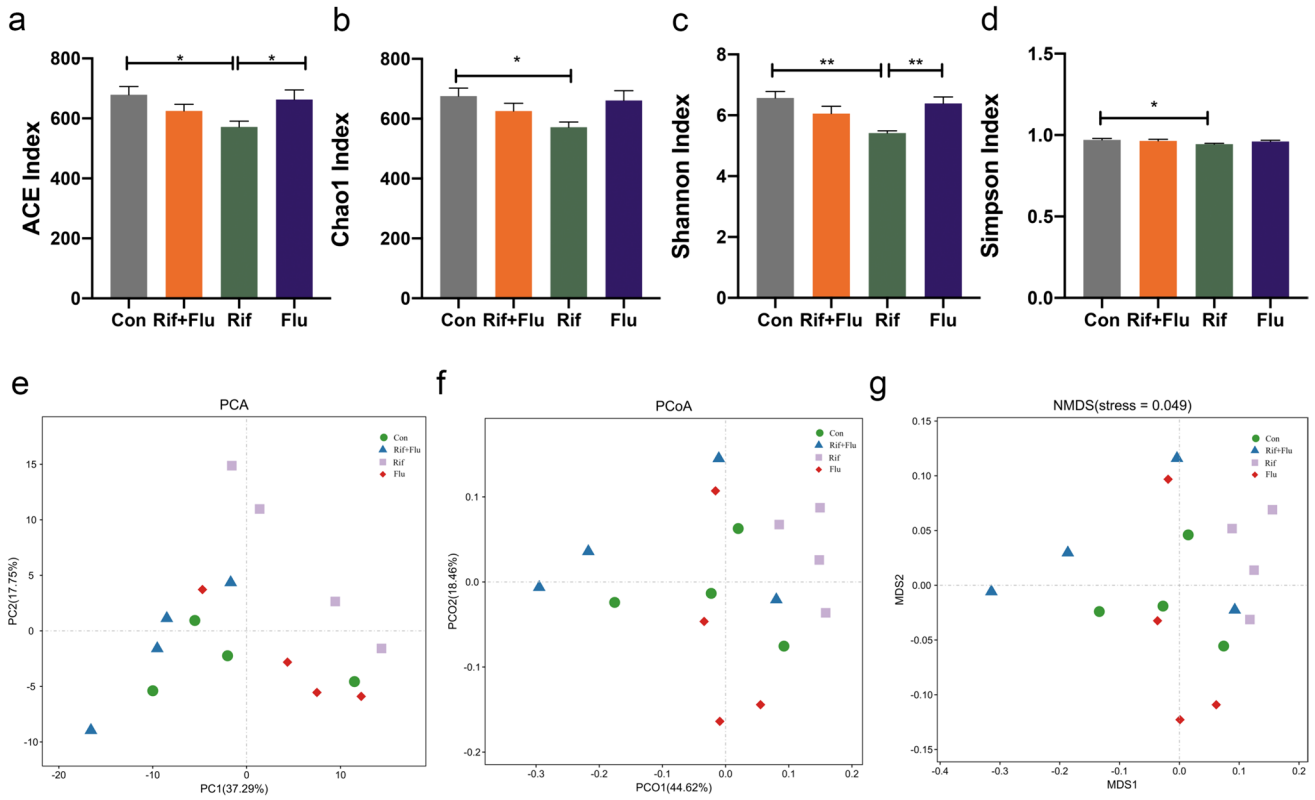

Fig. 2 Effects of influenza virus infection and rifaximin treatment on altered gut microbiota composition. **a** ACE index, **b** Chao1 index, **c** Shannon index, **d** Simpson index, **e** principal component analysis (PCA), (f) PCoA score plot, **g** nonmetric multidimensional scaling (NMDS) score plot based on the weight UniFrac score plot based on the OUT of the Con, Rif + Flu, Rif and Flu groups at day 4 post-infection. Con: Control group; Rif + Flu: Mice were treated with rifaximin after H1N1 infection.; Rif: Mice treated with rifaximin; Flu: Mice infected with H1N1. *$P < 0.05$; **$P < 0.01$; ***$P < 0.001$; ****$P < 0.0001$. All replicates are biological

microbial community profiles among the four groups were confirmed by PERMANOVA (R = 0.412, $p = 0.001$). Furthermore, UPGMA analysis showed that the Rif group exhibited significant dissimilarities compared to the other three groups in terms of fecal microbiota, consistent with the PCoA findings (Fig. S2a-S2b).

Abundance and significant difference between four groups at the phylum level The most prevalent bacteria found in mice feces at the phylum level were *Firmicutes* (Con: 51.91%, Rif + Flu: 59.77%, Rif: 38.92%, Flu: 59.07%), *Bacteroidetes* (Con: 38.16%, Rif + Flu: 33.45%, Rif: 53.66%, Flu: 35.16%), *Proteobacteria* (Con: 3.05%, Rif + Flu: 3.88%, Rif: 3.57%, Flu: 1.59%), and *Patescibacteria* (Con: 3.46%, Rif + Flu: 0.80%, Rif: 1.90%, Flu: 1.52%). *Actinobacteria*, *Epsilonbacteraeota*, and *Cyanobacteria* make up a smaller percentage in mice fecal microorganism (Fig. 3a-b). As shown in Fig. 3c, the Rif group had a lower relative abundance of *Firmicutes* compared to the Con, Rif + Flu, and Flu groups ($p = 0.012$–0.029). Additionally, in the Rif group, the prevalence of *Bacteroidetes* was higher compared to the Con, Rif + Flu, and Flu groups (Fig. 3d, $p = 0.004$–0.022). The abundance of *Actinobacteria* ($p = 0.001$–0.002) was higher in both the Rif group and Con group compared to the Rif + Flu group (Fig. 3g) and the abundance of *Patescibacteria* ($p = 0.003$–0.014) was higher in both the Rif + Flu group and Flu group compared to the Con group (Fig. 3f). In terms of *Proteobateria* abundance, there was no notable distinction observed among the four groups (Fig. 3e). The findings indicated that every group exhibited a distinct distribution pattern at the phylum level.

Abundance and significant difference between four groups at the genus level The microbial genus level results were shown in Fig. 4. As shown in Fig. 4a-b, we found that the dominant bacteria in fefal contents were *Lactobacillus* (Con: 11.88%, Rif + Flu: 6.17%, Rif: 17.77% Flu: 21.63%) and *Lachnospiraceae_NK4A136_group* (Con: 9.86%, Rif + Flu: 14.81%, Rif: 1.80% Flu: 6.79%). Afterwards, we employed LEfSe analysis to detect distinctive disparities in bacterial populations between the Flu and Con groups specifically at the genus level. As shown in Fig. 4c and Fig. S2c, the *Caproiciproducens*, *Mucispirillum*, was dominant in Flu group than in Con (*Caproiciproducens*, $p = 0.02$, LDA score = 3.12; *Mucispirillum*, $p = 0.02$, LDA score = 2.97). In the Con group, the prevalence of *Ruminococcaceae_UCG_013*, *Lachnoclostridium*, *Leucobacter*, and *Candidatus_Saccharimonas* was higher compared to the Flu group (*Ruminococcaceae_UCG_013*, $p = 0.02$, LDA score = 4.3; *Lachnoclostridium*, $p = 0.02$, LDA score = 3.59; *Leucobacter*, $p = 0.02$, LDA score = 3.08; *Candidatus_Saccharimonas*, $p = 0.02$, LDA score = 4.00). According to the wilcox test, the Con group had a significantly higher relative abundance of *Ruminococcaceae_UCG-013*, *Candidatus_Saccharimonas,* and *Lachnoclostridium* compared to the Flu group ($p = 0.03$). In the Rif + Flu group, the relative abundance of *Muribaculum*, *Erysipelatoclostridium,* and *Papillibacter* was higher compared to the Flu group (Fig. 4d, Fig. S2d, $p = 0.003$).

Effect of rifaximin on influenza a virus on altered gut microbiota metabolite composition

Functional prediction analysis of fecal microbiota using PICRUSt was conducted (Fig. S3a-S3b). The Rif + Flu group exhibited a higher predictive capacity for tryptophan metabolism in the KEGG level 3 pathway when compared to the Flu group. Additionally, "Tryptophan metabolism" was also increased in the Con group compared with the Rif group. These results suggested that the shifts of bacterial metabolic functions are induced by influenza virus as well as rifaximin supplement may improve the function of tryptophan metabolism in intestinal microorganisms. To further determine the changes in tryptophan metabolites in each group, targeted analysis of organic acid content was performed in fecal samples at day 4 post-influenza A virus infection (Fig. 5). The tryptophan levels experienced a notable rise (Fig. 5a, $p = 0.010$–0.044), indole-3-lactic acid (Fig. 5b, $p = 0.014$–0.020), 3-indole acrylic acid (Fig. 5c, $p = 0.008$–0.011), and indole propionic acid (Fig. 5d, $p = 0.001$–0.030) in the Rif + Flu, and Con group compared to Flu group, respectively. However, the content of indole-3-acetic acid, indole-3-carboxaldenhyde, and indole-3-glyoxylic acid in mouse feces showed no significant difference among the four treatment groups (Fig. 5e-g). According to the findings, the administration of rifaximin could mitigate the reduction in levels of tryptophan, indole-3-lactic acid, 3-indole acrylic acid, and indole propionic acid metabolites induced by influenza infection.

The AHR/IL-22/STAT-3 signaling pathways are involved in tryptophan metabolites mediated rifaximin-induced ILC3 activation

The analysis involved examining the distribution of lymphocytes and ILC3 cells in the lung, peripheral blood, and ileum based on the expression of particular transcription factors in ILC3 cells. As shown in Fig. 6a and Fig. S4a-S4b, we found that the number of lung lymphocytes was significantly increased in the Flu group compared to the Con group at day 4 post-influenza A virus infection (Fig. 6b and Fig. S4c). However, the number of peripheral blood lymphocytes was significantly decreased in the Flu group compared to the con group. Nevertheless, there was no notable distinction between the Con and Flu groups in terms of the quantity of lymphocytes in the ileum (Fig. 6c and Fig. S4d).

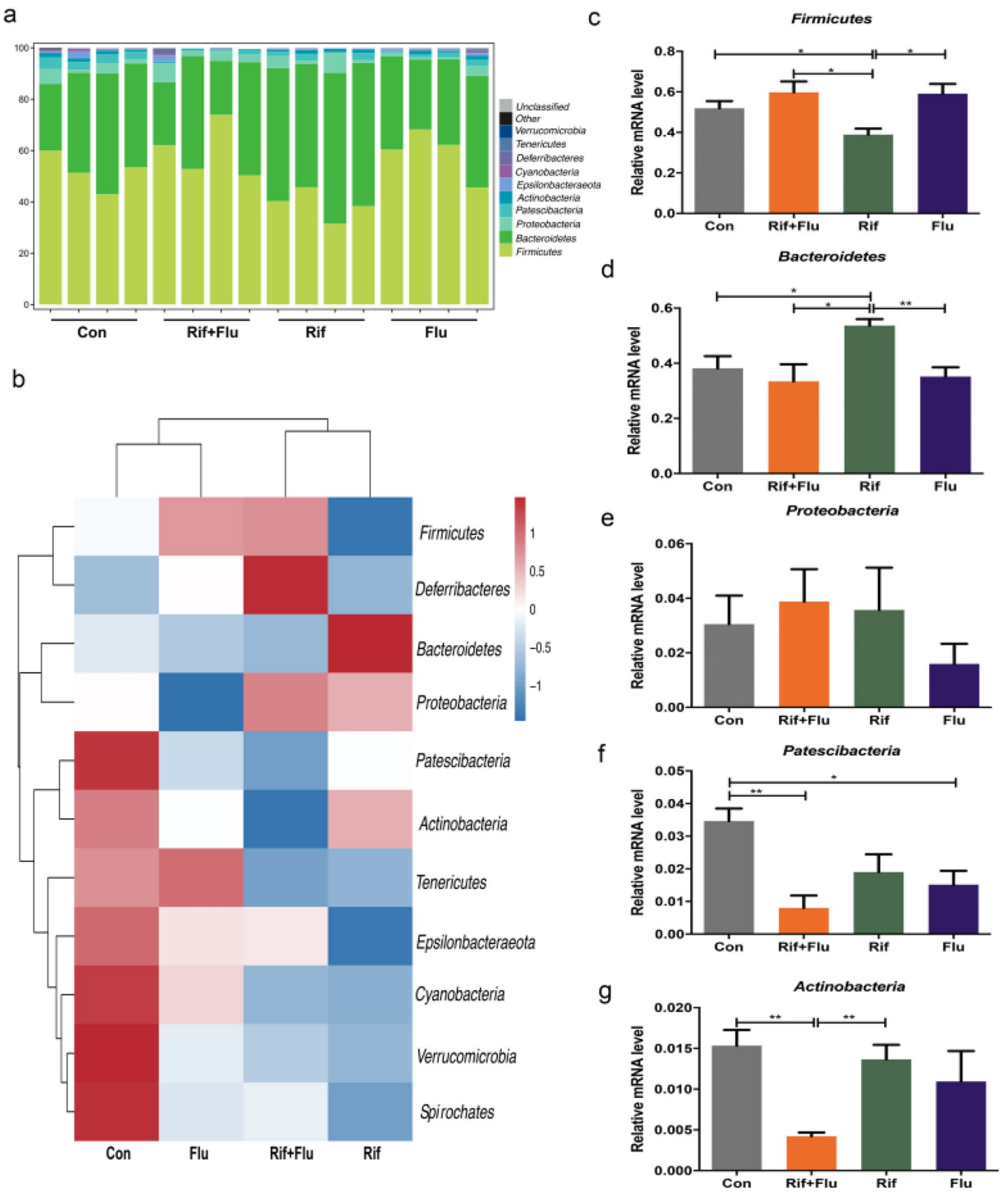

Fig. 3 Effects of influenza virus infection and rifaximin treatment on gut microbiota at the phylum level. **a** Relative contribution of the top 10 phyla in fecal microbe of Con, Rif + Flu, Rif and Flu groups, **b** Heatmap of the redundancy analysis-identified key phyla that were significantly altered in the fecal microbe of the Con, Rif + Flu, Rif and Flu groups, **c**-**g** Taxonomic profiles of the notably significantly different bacteria at the phylum level in the fecal microbe of the Con, Rif + Flu, Rif and Flu groups at day 4 post-infection. Con: Control group; Rif + Flu: Mice were treated with rifaximin after H1N1 infection.; Rif: Mice treated with rifaximin; Flu: Mice infected with H1N1. $^{*}P < 0.05$; $^{**}P < 0.01$; $^{***}P < 0.001$; $^{****}P < 0.0001$. All replicates are biological

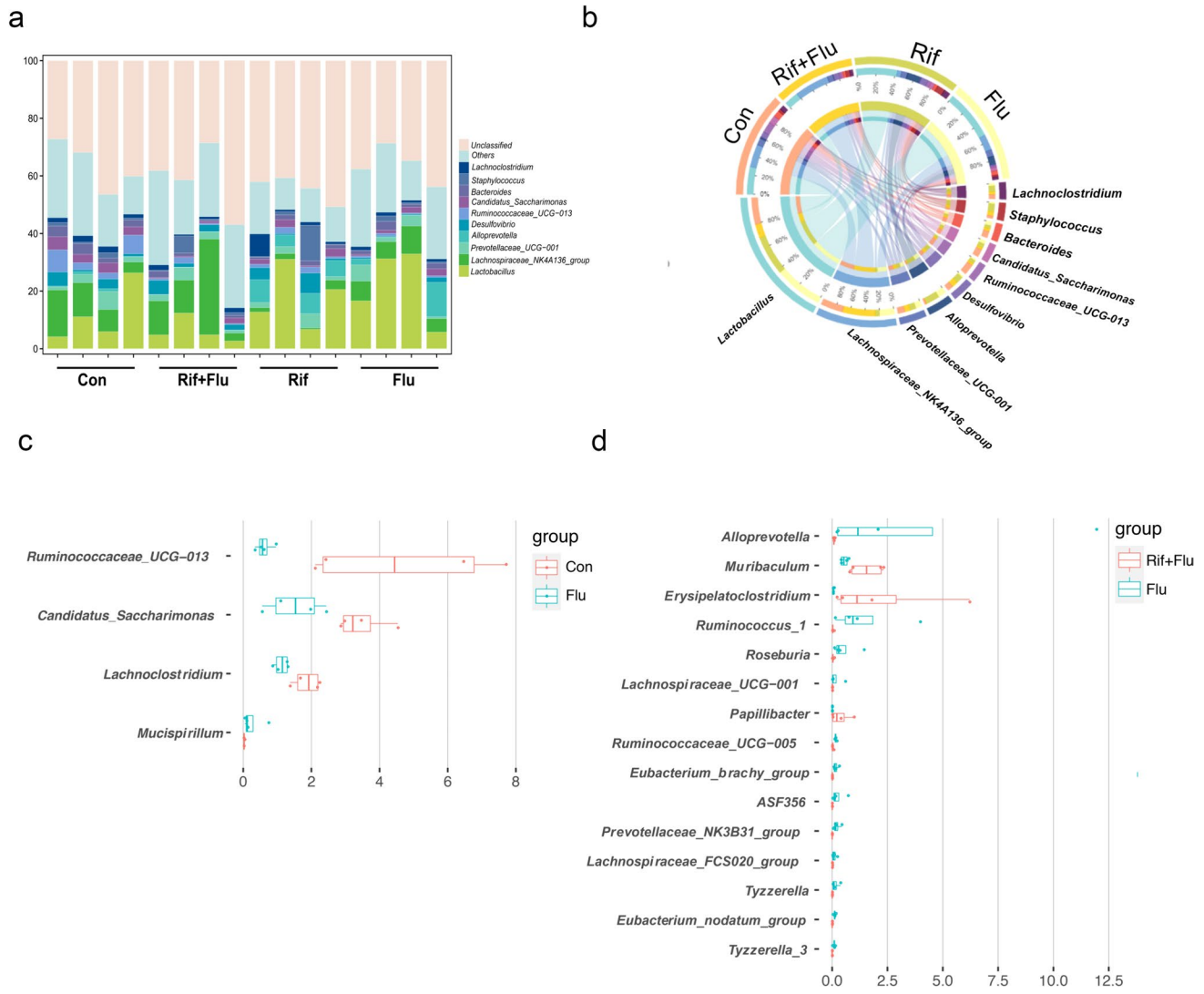

Fig. 4 Effects of influenza virus infection and rifaximin treatment on gut microbiota at the genus level. **a** Relative contribution of the top 10 genera in fecal microbe of Con, Rif + Flu, Rif and Flu groups, **b** Circos diagram of genus species in the fecal microbe of the Con, Rif + Flu, Rif and Flu groups, **c** Taxonomic profiles of the notably significantly different bacteria at the genus level in the fecal microbe of the Con and Flu groups, **d** Taxonomic profiles of the notably significantly different bacteria at the genus level in the fecal microbe of the Rif + Flu and Flu groups at day 4 post-infection. Con: Control group; Rif + Flu: Mice were treated with rifaximin after H1N1 infection.; Rif: Mice treated with rifaximin; Flu: Mice infected with H1N1. $^{*}P < 0.05$; $^{**}P < 0.01$; $^{***}P < 0.001$; $^{****}P < 0.0001$. All replicates are biological

Furthermore, according to Fig. 6d-f, the percentage of lung ILC3 cells significantly increased in the Rif + Flu group compared to the other three groups. However, rifaximin supplementation did not show significant changes in ILC3 cells in the intestine and peripheral blood. Moreover, IAV infection significantly decreased the quantity of ILC3 cells in the gastrointestinal tract. In contrast to the Flu group, the percentage of ILC3 cells in the peripheral blood of mice in the Flu + Rif group showed an increasing tendency, though no notable disparity was observed. Therefore, we speculate that rifaximin supplementation may promote the activation of ILC3 cells and facilitate their migration from the intestine to the lungs. Western blot was used to detect the presence of RORγ, a surface marker of ILC3 cells, in lung and intestine tissues. The findings were consistent with the outcomes of flow cytometry. The level of RORγ protein expression in the lung tissue of mice in the Rif + Flu group showed a notable increase compared to the Con group (Fig. 6g). In comparison to the Con group, there was also a noticeable rise in RORγ protein expression in the lungs of mice infected with influenza virus. However, there was no significant variation in the expression of RORγ protein in the intestine of mice across the four treatment groups (Fig. 6h). These results indicated that rifaximin supplementation can increase the

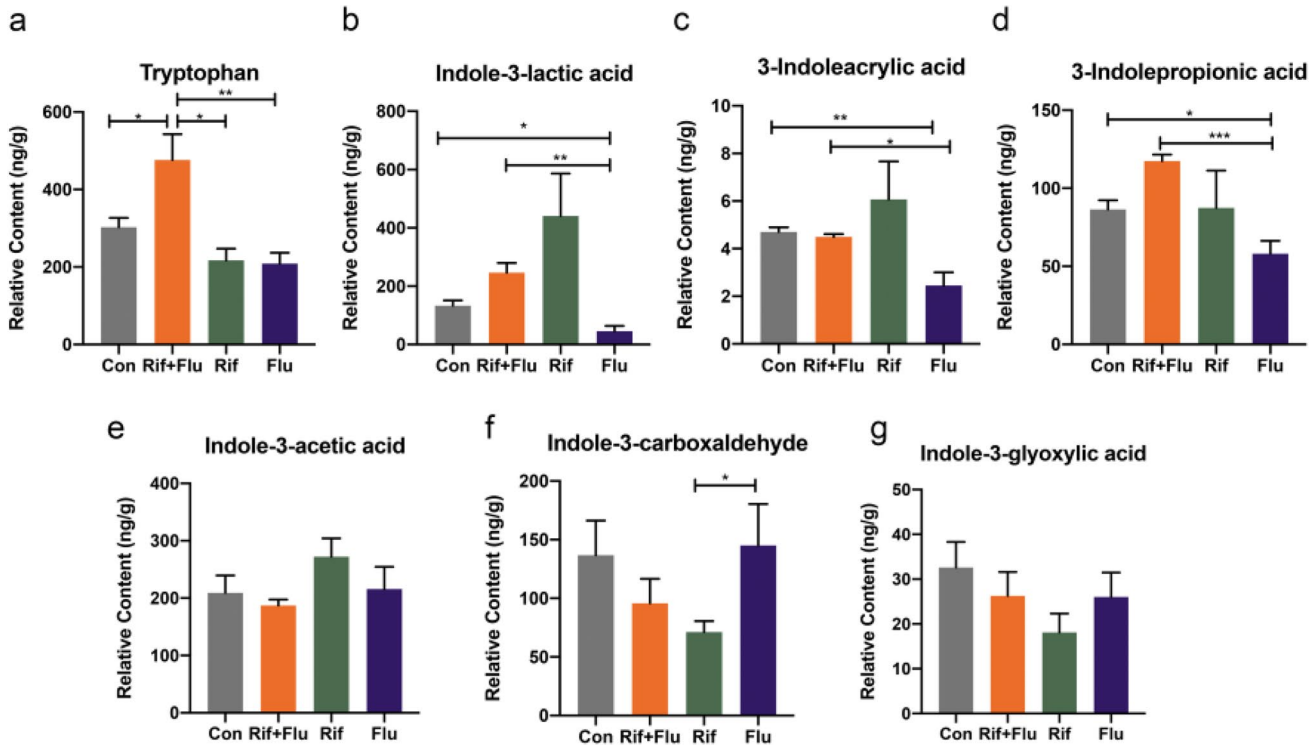

Fig. 5 Effects of influenza virus infection and rifaximin treatment on altered gut microbiota tryptophan metabolite composition. **a** The relative abundance of tryptophan, **b** Indole-3-lactic acid, **c** 3-indoleacrylic acid, **d** 3-indolepropionic acid, **e** Indole-3-acetic acid, **f** Indole-3-carboxaldehyde, and **g** Indole-3-glyoxylic acid in the Con, Rif + Flu, Rif and Flu groups in the feces microbiota at day 4 post-infection. Con: Control group; Rif + Flu: Mice were treated with rifaximin after H1N1 infection.; Rif: Mice treated with rifaximin; Flu: Mice infected with H1N1. $^{*}P < 0.05$; $^{**}P < 0.01$; $^{***}P < 0.001$; $^{****}P < 0.0001$. All replicates are biological

activation of ILC3 cells, potentially through its effects on tryptophan metabolites.

Next, we aimed to explore the signaling pathways through which tryptophan metabolites promote the activation of ILC3 cells. Tryptophan metabolites can be recognized by the AhR on the surface of ILC3 cells, enhancing mucosal immunity. Therefore, we examined the expression levels of AhR, the critical rate-limiting enzyme IDO-1 in tryptophan metabolism, and STAT-3 in the mouse ileum. Compared with the Flu group, the Rif + Flu group exhibited significant up-regulation in the expression of AhR (Fig. 7a, d), IDO-1 (Fig. 7b, e), and STAT-3 (Fig. 7c, f) in the ileum. Additionally, IL-22 is a primary product of activated ILC3 cells. Therefore, we assessed the mRNA expression of the chemokine *CCL20* in ILC3 cells in the lungs. As shown in Fig. 7g-h, the mRNA levels and concentrations of CCL20 in the lungs were significantly higher in both the Flu group and Rif + Flu group compared to the Con group. Conversely, the concentration of CCL20 in peripheral blood significantly decreased in the Flu group and Rif + Flu group compared to the Con group (Fig. 7i). These findings suggest that rifaximin treatment can activate ILC3 cells by restoring tryptophan metabolism, leading to IL-22 production and enhanced resistance to IAV infection.

Effect of rifaximin on influenza A virus altered the barrier structure of the lung

As shown in Fig. 8a-d, the western blot results indicated a significant reduction in claudin-1 and zo-1 protein levels in the lung of the Flu group compared to the Con group (Fig. 8a-d). Furthermore, the Rif + Flu group exhibited notably elevated expression of zo-1 protein compared to the Flu group. However, there was no significant difference in the level of occludin protein among the four groups. These findings suggest that rifaximin treatment can alleviate lung barrier damage induced by IAV infection.

The qPCR findings indicated a significant increase in *SP-B* mRNA in the Flu group, while there was no notable distinction between the Con group and the Rif + Flu group (Fig. 8e). These results from the determination of tight junction protein-related gene showed a significant decrease in *claudin-1* mRNA in the lungs of Rif + Flu and Flu groups. Furthermore, the expression of *IGF-1* mRNA in the Rif + Flu group exhibited a significant increase compared to the other groups, as depicted in Fig. 8h. These findings suggested that infection with the H1N1 virus enhanced *SP-B* gene expression while suppressing proteins involved in tight junctions. After activating ILC3 cells and enhancing the expression

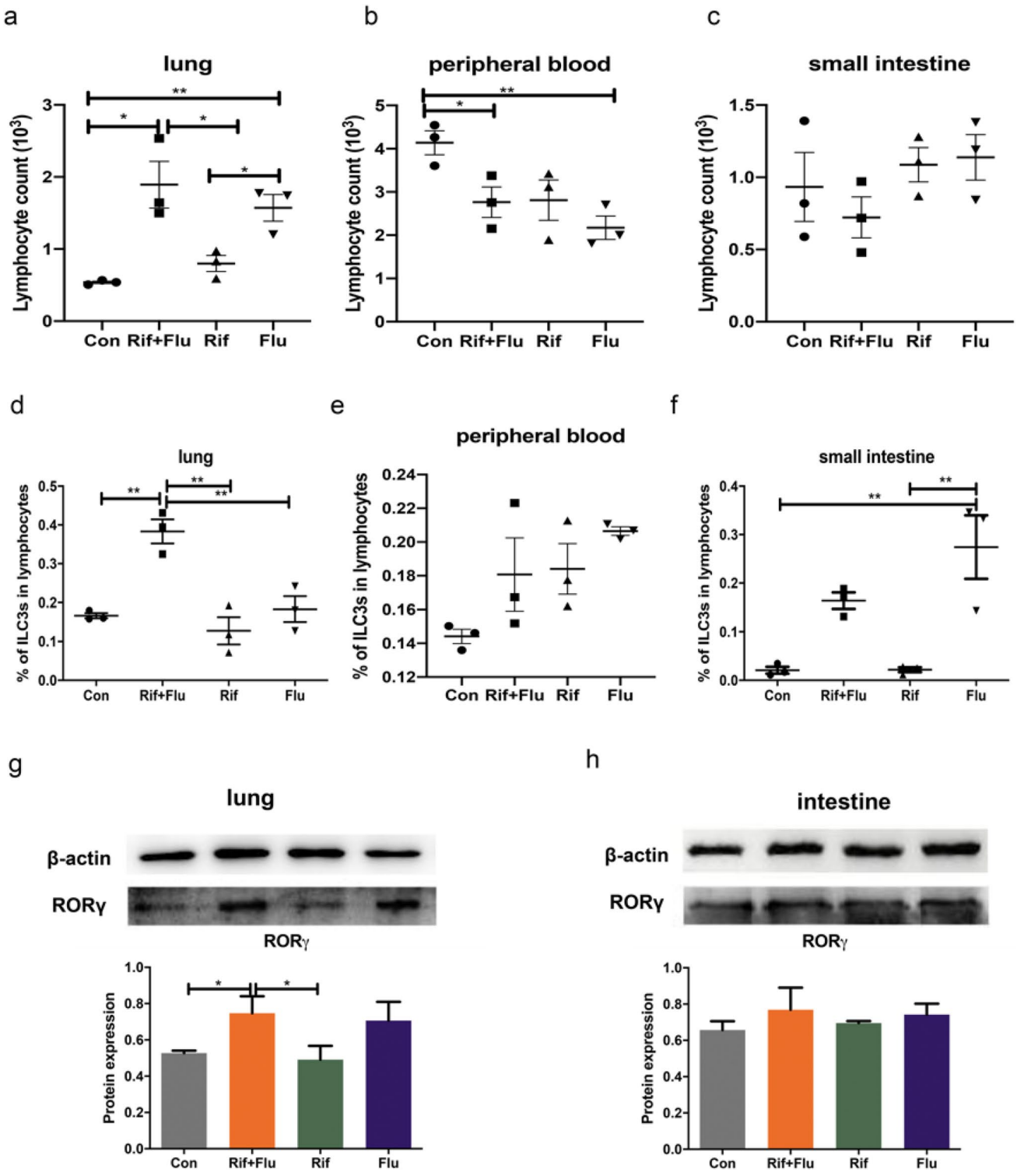

Fig. 6 Effects of influenza virus infection and rifaximin treatment on the number of lymphocytes and ILC3s in the lung, peripheral blood and small intestine. **a** Comparison of lung lymphocyte counts between the four groups, **b** Comparison of peripheral blood lymphocyte counts between the four groups, **c** Comparison of small intestine lymphocyte counts, **d** The ratio of lung ILC3s to lymphocyte numbers, **e** The ratio of peripheral blood ILC3s to lymphocyte numbers, **f** The ratio of small intestine ILC3s to lymphocyte numbers, **g** Expression of RORγ protein in lung, **h** Expression of RORγ protein in intestine between the Con, Rif + Flu, Rif and Flu groups at day 4 post-infection. Con: Control group; Rif + Flu: Mice were treated with rifaximin after H1N1 infection.; Rif: Mice treated with rifaximin; Flu: Mice infected with H1N1. $^{*}P < 0.05$; $^{**}P < 0.01$; $^{***}P < 0.001$; $^{****}P < 0.0001$. All replicates are biological

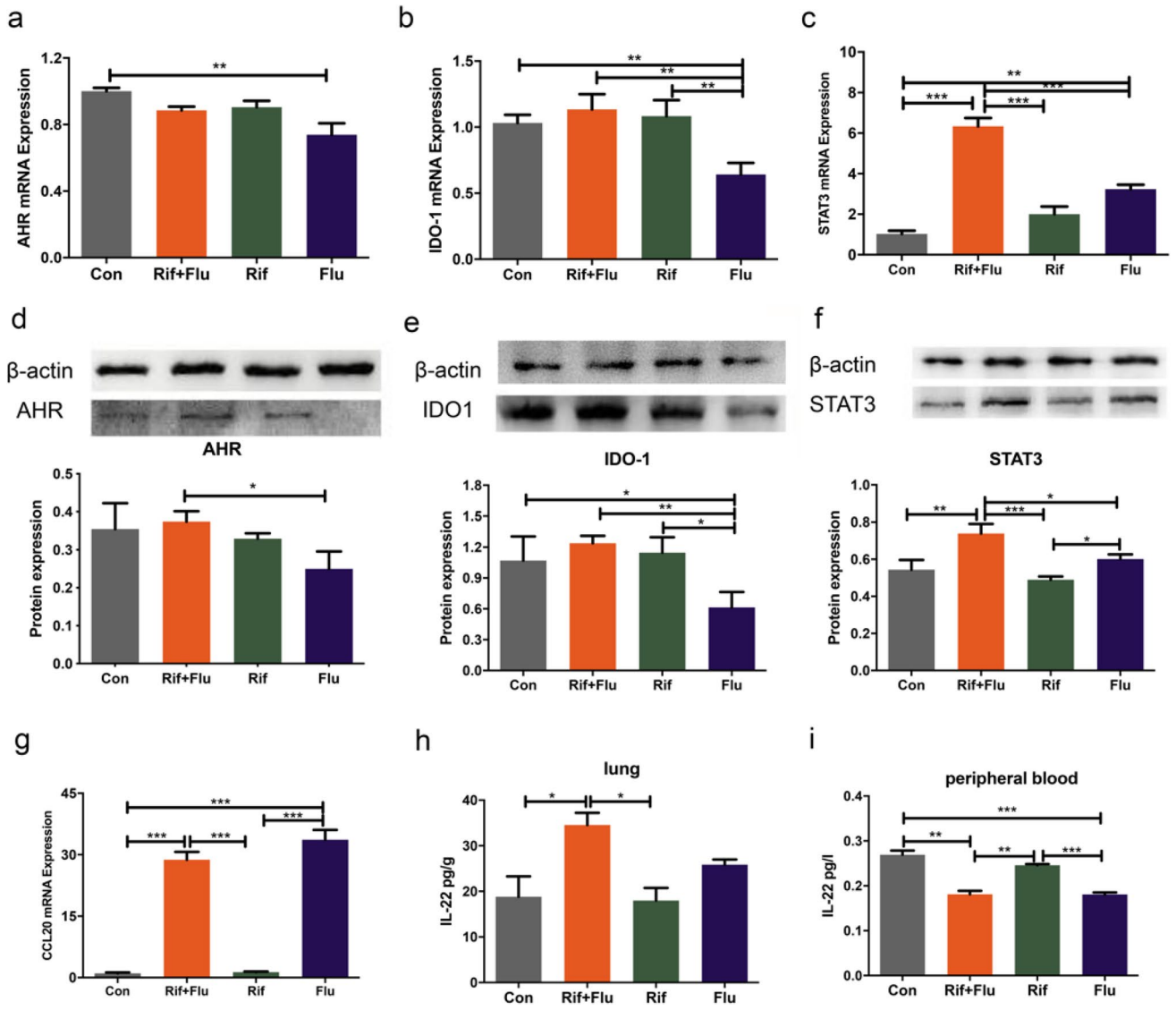

Fig. 7 Expression of genes and proteins related to ILC3 signaling pathway. **a** *AHR* mRNA level in the ileum, **b** *IDO*1 mRNA level in the ileum, **c** *STAT3* mRNA level in the lung, **d** AHR protein expression in the ileum, **e** IDO1 protein expression in the ileum, **f** STAT3 protein expression in the lung, **g** *CCL20* mRNA level in the lung, **h** IL-22 concentrations in the lung, **i** IL-22 concentrations in the peripheral blood between the Con, Rif + Flu, Rif and Flu groups at day 4 post-infection. Con: Control group; Rif + Flu: Mice were treated with rifaximin after H1N1 infection.; Rif: Mice treated with rifaximin; Flu: Mice infected with H1N1. $^{*}P < 0.05$; $^{**}P < 0.01$; $^{***}P < 0.001$; $^{****}P < 0.0001$. All replicates are biological

of genes related to damage repair, we analyzed the variations in *IFN-γ*, *ISG-15*, and *viperin* genes among distinct treatment groups. As shown in Fig. 8h-i, mRNA levels of *IFN-γ*, *ISG-15*, and *viperin* genes were markedly elevated in the Flu group and Rif + Flu group. Moreover, expression of *IFN-γ* and *ISG-15* was notably higher in the Rif + Flu group compared to the Flu group. Additionally, the mRNA of the innate immune protein gene *IFITM3* decreased in the Flu group but significantly increased in the Rif + Flu group (Fig. 8l). These findings suggest that the initial phase of influenza virus infection is significantly influenced by the innate immune response, and rifaximin exhibits a beneficial impact on innate immunity.

Discussion

When the influenza virus infects a host, large numbers of neutrophils accumulate in lung tissue, causing inflammation and damage to the lungs. Meanwhile, influenza viruses can metastasize to non-lung tissue via immune cells, leading to serious complications (Peteranderl et al. 2016). Hence,

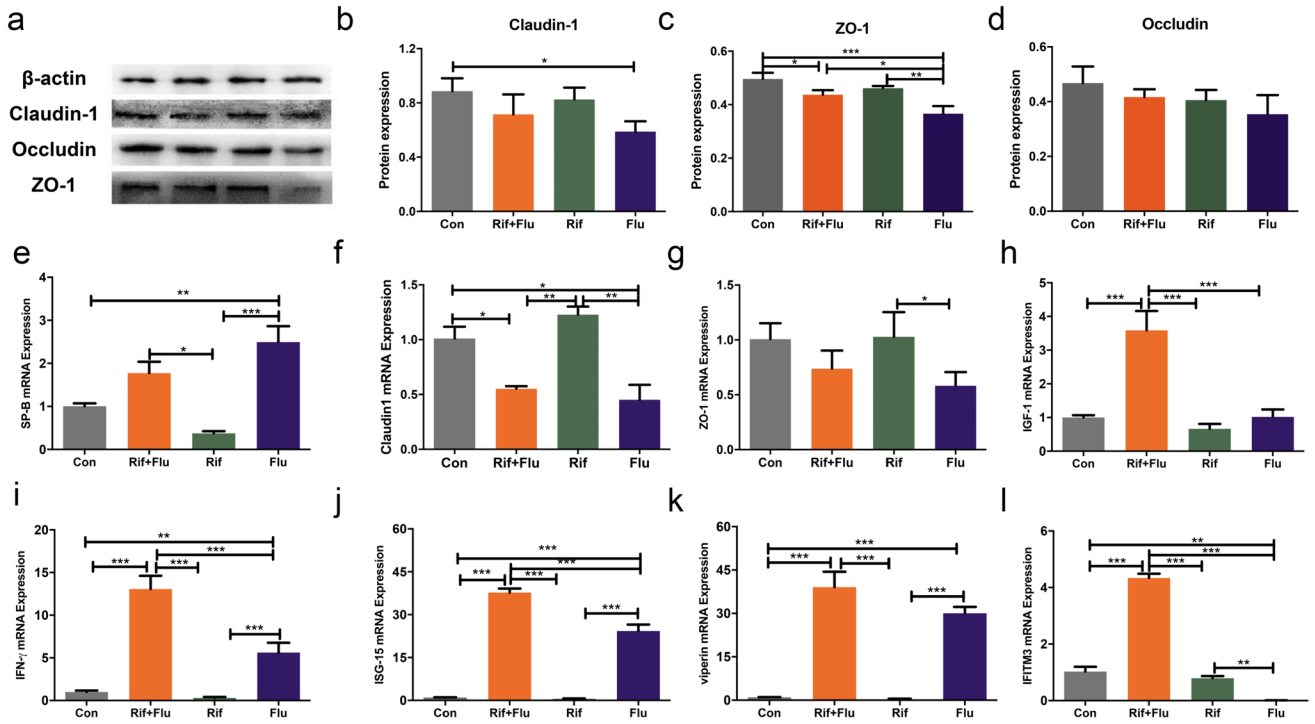

Fig. 8 Effect of rifaximin on influenza A virus altered the barrier structure of the lung. **a**-**d** Claudin-1, occludin, and zo-1 protein expression, **e** *SP-B* mRNA level, **f** Claudin-1 mRNA level, **g** *zo-1* mRNA level, **h** *IGF-1* mRNA level, **i** *IFN-γ* mRNA level, **j** *ISG-15* mRNA level, **k** *Viperin* mRNA level, **l** *IFITM3* mRNA level in the Con, Rif + Flu, Rif and Flu groups at day 4 post-infection. Con: Control group; Rif + Flu: Mice were treated with rifaximin after H1N1 infection.; Rif: Mice treated with rifaximin; Flu: Mice infected with H1N1. $^{*}P < 0.05$; $^{**}P < 0.01$; $^{***}P < 0.001$; $^{****}P < 0.0001$. All replicates are biological

it is highly important to uphold the structural integrity of the lungs as a means to combat influenza virus transmission and decrease illness and death rates. Our results showed that influenza infection causes inflammation and exudation of lung tissue and increased lung mass. The analysis of the morphology revealed that during the initial phase of influenza virus infection, there was a rupture in the alveolar septum, infiltration of inflammatory cells, and exudation of red blood cells. These findings suggest that the immune barrier in the lungs has been compromised (Merga et al. 2014). Furthermore, our research discovered that the intestinal lumen of the colon contracted and became congested in mice infected with the influenza virus. The H&E staining revealed that infection with the influenza virus resulted in structural damage to the colon and intestines, leading to a decrease in the length of intestinal glands, crypt atrophy, a decrease in goblet cells, epithelial cell necrosis, and infiltration of inflammatory cells. PCR detection results indicated that there was no viral RNA expression in colon tissue, suggesting that colonic mucosal barrier damage is not directly related to influenza virus. The results of our research are additionally backed by prior studies which discovered that H9N2 IAV infection can disturb the ileal mucosal barrier in BALB/c mice, resulting in disruption of gut microbiota and ultimately leading to bacterial translocation (Lu et al. 2019). However, the damaging effects of the influenza virus on the lungs and intestines were reversed by rifaximin supplementation. The findings suggested that structural growth was considerably hindered in the respiratory system and gastrointestinal tract following infection with the IAV. However, the addition of rifaximin greatly improved this condition.

The homeostasis of intestinal commensal bacteria is increasingly affected by influenza virus infection, as evidenced by a growing number of clinical cases and mouse models. A previous study found that the relative abundance of *Bacteroides* in the small intestine of mice infected with H5N1 was significantly reduced while the probiotic *Lactobacillus* was significantly increased (Groves et al. 2018). Consistent with prior research, our findings indicated that following infection with the influenza virus, the proportion of *Ruminococcaceae_UCG_013, Lachnoclostridium, Leucobacter,* and *Candidatus_Saccharimonas* was notably reduced in comparison to the Con group. Nevertheless, following infection with the influenza virus and administration of rifaximin, mice exhibited enhanced levels of *Muribaculum, Erysipelatoclostridium* and *Papillibacter*. *Muribaculum*, is the first genus found in the *Muribaculaceae* and has been reported to be associated with a better response

to immunotherapy (Uribe-Herranz et al. 2018) and tryptophan metabolism (Huang et al. 2022). Notably, we observed a greater prevalence of genes associated with tryptophan metabolism that were enriched in the Rif + Flu group compared to the Flu group. These results suggested that administering rifaximin following influenza virus infection may boost the tryptophan metabolic pathway and the production of tryptophan-related metabolites by intestinal microorganisms. Zhang and his colleagues discovered in 2021 that the utilization of tryptophan metabolites can serve as signaling molecules, triggering the innate immune response in the intestinal mucosa, thereby initiating inflammation at an early stage and safeguarding the balance of the intestinal microbiota (Zhang et al. 2021).

In order to further confirm our hypothesis, we employed LC–MS, a technique combining liquid chromatography and tandem mass spectrometry, to identify the metabolites associated with the metabolic pathway of tryptophan. The results illustrated that the contents of tryptophan, indole-3-lactic acid, 3-indoleacrylic acid, and 3-indolepropionic acid in the feces of the Flu group were significantly decreased compared with the Con group, indicating that influenza infection interfered with the normal intestinal flora and had a negative impact on the body's tryptophan metabolism. However, the treatment with rifaximin relieved the decrease of tryptophan, indole-3-lactic acid, 3-indoleacrylic acid, and 3-indolepropionic acid metabolites caused by influenza infection. Indole-3-lactic acid, a metabolite derived from tryptophan, plays a crucial role in maintaining intestinal immune balance by influencing the differentiation of T cells and activating natural immunity through the AHR signaling pathway (Cervantes-Barragan et al. 2017). In addition, tryptophan (Kepert et al. 2017), 3-indoleacrylic acid (Wlodarska et al. 2017), and 3-indolepropionic acid (Venkatesh et al. 2014) all can enhance the activity of immune cells in the intestinal lamina propria and strengthen intestinal barrier function. The above studies indicated that rifaximin treatment can enhance the metabolism of tryptophan in intestinal microorganisms, but whether rifaximin can promote IL-22 secretion and thus regulate intestinal mucosal immunity by regulating AhR activation remains to be further explored.

Lymphocytes play a crucial role in assessing the body's immune response in clinical evaluations. When pathogens infect the host, it will lead to systemic changes in the number of lymphocytes by activating the immune response of the body. Hence, the identification of immune cell categorization and variations in lymphocyte subsets is crucial for diagnosing and distinguishing diseases, assessing the state, and predicting the outcome. Our results confirmed that H1N1 virus infected mice showed an increase in lymphocyte in the lungs at the early stage (Fig. 6b), and a significant decrease in peripheral blood (Fig. 6c). There was no significant change in lymphocytes in the intestine, indicating that there was no immune response caused by the invasion of influenza virus in the intestine on the 4th day after infection. ILC3 cells occupy an important function in innate immunity. The relationship between ILC3 cells and intestinal commensal bacteria is strongly connected (Mortha et al. 2014). By producing cytokines, ILC3 cells play a crucial role in maintaining immunity and homeostasis, while also contributing to the control of the overall immune response (Ardain et al. 2019; Sonnenberg et al. 2011a, b). RORγ is a specific transcription factor of ILC3 cells. Our results showed that ILC3 cells in the mouse ileum increased significantly after influenza infection (Fig. 6g), and the number of ILC3 cells in the lung and peripheral blood increased slightly (Fig. 6e-f). The percentage of ILC3 cells in the mouse lungs in the Rif + Flu group showed a significant increase, although it was lower compared to the increase observed in the intestinal region of the Flu group. This might be due to the response speed of microorganisms to ILC3 cells.

There are multiple pathways to activate ILC3 cells in the intestine. The tryptophan metabolite- indole organic acid can be directly activated by binding to AhR on ILC3 cells (Gronke et al. 2019). By combining the findings from LC–MS analysis, the investigation determined the AhR pathway in ILC3 cells. Interestingly, a notable decrease in the expression of IDO1, a crucial enzyme that regulates AhR and tryptophan metabolism, was observed in the Flu group. These results suggested that influenza virus infection impacts the activation of ILC3 cells mediated by microorganisms. However, this did not align with the rise in the quantity of ILC3 cells in the gut, necessitating further investigation into the activation mechanism of ILC3 cells during influenza infection. Rifaximin drug treatment maintained the expression of AhR and IDO1 proteins in the intestine, suggesting that the tryptophan metabolism pathway associated with intestinal microbes was stabilized to ensure the activity of ILCs in the intestine and resist pathogen invasion. ILC3 cells are the main source of IL-22 at the early stage of infection (Sonnenberg et al. 2011a, b). IL-22 is generated via the STAT3 signaling pathway following the activation of ILC3 cells, and this pathway is crucial for preserving the immune barrier. During the experiment, there was a notable rise in the IL-22 levels in the lung tissue of mice infected with influenza, while a significant decrease in IL-22 was observed in the peripheral blood. Following the administration of rifaximin, there was an augmentation in IL-22 release within the pulmonary tissue of mice, with the predominant presence of ILC3 cells observed in the intestinal lamina propria. The increase in the amount of ILC3 cells and IL-22 secretion in the lung tissue was suspected to be related to cell migration. LTi + ILC3 cells express CCR6, which is regulated by the chemokine CCL20 and has the ability to migrate. Measurement was conducted to determine the level of *CCL20* gene expression in lung tissue, and the results

revealed a significant increase in *CCL20* mRNA expression in the lungs of the Flu group, suggesting the migration of ILC3 cells. The Rif + Flu group exhibited a notably elevated expression of the *CCL20* gene compared to the Flu group, aligning with the findings on the content of ILC3 cells in the lungs. This indicates that preserving the structure and function of intestinal microbes promotes the migratory response of ILC3 cells and sustains mucosal immunity in the lungs.

The host defense and tissue repair functions of ILC3 cells are mainly mediated by IL-22. IL-22 is essential for maintaining lung structure and function after influenza infection, and it also helps prevent secondary bacterial pneumonia (Kudva et al. 2011). The detection of STAT3 and crucial immune barrier genes in lung tissue confirmed that the Rif + Flu group, which had a high IL-22 expression, exhibited notably elevated STAT3 expression compared to the Flu group. Consequently, STAT3 stimulated the upregulation of *IGF-1* and *SP-B* genes, facilitating the recovery of lung damage. IL-22 helps promote the expression of tight junction proteins (Barthelemy et al. 2018). This investigation verified that the elevated secretion of IL-22 could mitigate the harm caused by influenza virus infection to the tight junction proteins Claudin-1 and ZO-1. In addition, the high expression of *IGF-1* and *MUC2* mRNA verified that IL-22 enhances epithelial cell metabolism and guarantees mucin secretion. Prior research has discovered that IL-22 has a significant function in triggering the antiviral innate immune reaction (Swaim et al. 2020), inhibiting the replication of the influenza virus (Waheed and Freed 2007), and killing the target cells of viral infection (Kenney et al. 2019). Additionally, our research revealed that IL-22 can enhance the production of antiviral genes *IFN-γ*, *ISG-15*, *viperin*, and *IFITM3* during the initial phase of influenza virus infection, further confirming the previous perspective.

To summarize, rifaximin enhanced the activation of ILC3 cells by stabilizing the composition of the gut microbiota, facilitating their migration to the lungs, and subsequently inducing the production of IL-22 through the tryptophan metabolic pathway of commensal bacteria residing in the intestines. IL-22 then aided in repairing the damage caused by influenza infection during the initial phase, contributing to the regulation of the innate immune response against viruses and defending against viral invasion. Therefore, rifaximin has the potential to become an adjuvant drug for the treatment of influenza through the intestinal symbiotic bacteria/tryptophan metabolic/ILC3 cells/AHR/STAT3 pathway.

Supplementary Information The online version contains supplementary material available at https://doi.org/10.1007/s00253-024-13280-6.

Acknowledgements The authors would like to thank all members of the animal neurobiology laboratory.

Author's contributions The study design was contributed by JS and YC; funding was obtained by JS, JP, and JX; the experiments were performed by YC, WQ, LC, and LL; data analysis was conducted by YZ, YC, and HL; the manuscript was written by YZ and YC. The article was contributed to by all authors and the submitted version was approved by them.

Funding This study was supported by the Xinjiang Uygur Autonomous Region Major Science and Technology Project—Xinjiang Animal Disease Prevention and Control System Quality Improvement Project (2023A02007) and the Xinjiang Uygur Autonomous Region 'Heavenly Lake Talent' Recruitment Program Project.

Data availability The sequencing data we generated were deposited in the NCBI Sequence Read Archive (SRA) under accession numbers from SAMN37928519 to SAMN37928534 in PRJNA1031154. The data that support the findings of this study are available from the corresponding author upon reasonable request.

Declarations

Ethics approval and consent to participate The mice were handled humanely according to the rules described by the Animal Ethics Procedures and Guidelines of the People's Republic of China and Institutional Animal Care and Use Committee of Nanjing Agricultural University [SYXK (Su) 2017–0007].

Competing interests The authors have declared no conflict of interest.

References

Ardain A, Porterfield JZ, Kloverpris HN, Leslie A (2019) Type 3 ILCs in lung disease. Front Immunol 10:92. https://doi.org/10.3389/fimmu.2019.00092

Barthelemy A, Sencio V, Soulard D, Deruyter L, Faveeuw C, Le Goffic R, Trottein F (2018) Interleukin-22 immunotherapy during severe influenza enhances lung tissue integrity and reduces secondary bacterial systemic invasion. Infect Immun 86(7). https://doi.org/10.1128/IAI.00706-17

Cervantes-Barragan L, Chai JN, Tianero MD, Di Luccia B, Ahern PP, Merriman J, Cortez VS, Caparon MG, Donia MS, Gilfillan S, Cella M, Gordon JI, Hsieh CS, Colonna M (2017) *Lactobacillus reuteri* induces gut intraepithelial CD4(+)CD8α(+) T cells. Science 357(6353):806–810. https://doi.org/10.1126/science.aah5825

Chen Y, Jiang Z, Lei Z, Ping J, Su J (2021) Effect of rifaximin on gut-lung axis in mice infected with influenza A virus. Comp Immunol Microbiol Infect Dis 75:101611. https://doi.org/10.1016/j.cimid.2021.101611

Dumas A, Bernard L, Poquet Y, Lugo-Villarino G, Neyrolles O (2018) The role of the lung microbiota and the gut-lung axis in respiratory infectious diseases. Cell Microbiol 20(12):e12966. https://doi.org/10.1111/cmi.12966

DuPont HL (2016a) Introduction: understanding mechanisms of the actions of rifaximin in selected gastrointestinal diseases. Aliment Pharmacol Ther 43(Suppl 1):1–2. https://doi.org/10.1111/apt.13406

DuPont HL (2016b) Review article: the antimicrobial effects of rifaximin on the gut microbiota. Aliment Pharmacol Ther 43(Suppl 1):3–10. https://doi.org/10.1111/apt.13434

Gatta L, Scarpignato C (2017) Systematic review with meta-analysis: rifaximin is effective and safe for the treatment of small intestine bacterial overgrowth. Aliment Pharmacol Ther 45(5):604–616. https://doi.org/10.1111/apt.13928

Gronke K, Hernandez PP, Zimmermann J, Klose CSN, Kofoed-Branzk M, Guendel F, Witkowski M, Tizian C, Amann L, Schumacher F, Glatt H, Triantafyllopoulou A, Diefenbach A (2019) Interleukin-22 protects intestinal stem cells against genotoxic stress. Nature 566(7743):249–253. https://doi.org/10.1038/s41586-019-0899-7

Groves HT, Cuthbertson L, James P, Moffatt MF, Cox MJ, Tregoning JS (2018) Respiratory disease following viral lung infection alters the murine gut microbiota. Front Immunol 9:182. https://doi.org/10.3389/fimmu.2018.00182

Hause BM, Collin EA, Liu R, Huang B, Sheng Z, Lu W, Wang D, Nelson EA, Li F (2014) Characterization of a novel influenza virus in cattle and swine: proposal for a new genus in the Orthomyxoviridae family. mBio 5(2):e00031-14. https://doi.org/10.1128/mBio.00031-14

Huang J, Liu D, Wang Y, Liu L, Li J, Yuan J, Jiang Z, Jiang Z, Hsiao WW, Liu H, Khan I, Xie Y, Wu J, Xie Y, Zhang Y, Fu Y, Liao J, Wang W, Lai H, Shi A, Cai J, Luo L, Li R, Yao X, Fan X, Wu Q, Liu Z, Yan P, Lu J, Yang M, Wang L, Cao Y, Wei H, Leung EL (2022) Ginseng polysaccharides alter the gut microbiota and kynurenine/tryptophan ratio, potentiating the antitumour effect of antiprogrammed cell death 1/programmed cell death ligand 1 (anti-PD-1/PD-L1) immunotherapy. Gut 71(4):734–745. https://doi.org/10.1136/gutjnl-2020-321031

Keely S, Talley NJ, Hansbro PM (2012) Pulmonary-intestinal cross-talk in mucosal inflammatory disease. Mucosal Immunol 5(1):7–18. https://doi.org/10.1038/mi.2011.55

Kenney AD, McMichael TM, Imas A, Chesarino NM, Zhang L, Dorn LE, Wu Q, Alfaour O, Amari F, Chen M, Zani A, Chemudupati M, Accornero F, Coppola V, Rajaram MVS, Yount JS (2019) IFITM3 protects the heart during influenza virus infection. Proc Natl Acad Sci U S A 116(37):18607–18612. https://doi.org/10.1073/pnas.1900784116

Kepert I, Fonseca J, Müller C, Milger K, Hochwind K, Kostric M, Fedoseeva M, Ohnmacht C, Dehmel S, Nathan P, Bartel S, Eickelberg O, Schloter M, Hartmann A, Schmitt-Kopplin P, Krauss-Etschmann S (2017) D-tryptophan from probiotic bacteria influences the gut microbiome and allergic airway disease. J Allergy Clin Immunol 139(5):1525–1535. https://doi.org/10.1016/j.jaci.2016.09.003

Kudva A, Scheller EV, Robinson KM, Crowe CR, Choi SM, Slight SR, Khader SA, Dubin PJ, Enelow RI, Kolls JK, Alcorn JF (2011) Influenza A inhibits Th17-mediated host defense against bacterial pneumonia in mice. J Immunol 186(3):1666–1674. https://doi.org/10.4049/jimmunol.1002194

Liu L, Chen G, Huang S, Wen F (2023) Receptor binding properties of neuraminidase for influenza a virus: an overview of recent research advances. Virulence 14(1):2235459. https://doi.org/10.1080/21505594.2023.2235459

Lu H, Zhang L, Xiao J, Wu C, Zhang H, Chen Y, Hu Z, Lin W, Xie Q, Li H (2019) Effect of feeding Chinese herb medicine ageratum-liquid on intestinal bacterial translocations induced by H9N2 AIV in mice. Virol J 16(1):24. https://doi.org/10.1186/s12985-019-1131-y

Luo M, Xie P, Deng X, Fan J, Xiong L (2023) Rifaximin ameliorates loperamide-induced constipation in rats through the regulation of gut microbiota and serum metabolites. Nutrients 15(21):4502. https://doi.org/10.3390/nu15214502

Martinu T, McManigle WC, Kelly FL, Nelson ME, Sun J, Zhang HL, Kolls JK, Gowdy KM, Palmer SM (2019) IL-17A contributes to lung fibrosis in a model of chronic pulmonary graft-versus-host disease. Transplantation 103(11):2264–2274. https://doi.org/10.1097/TP.0000000000002837

Merga Y, Campbell BJ, Rhodes JM (2014) Mucosal barrier, bacteria and inflammatory bowel disease: possibilities for therapy. Dig Dis 32(4):475–483. https://doi.org/10.1159/000358156

Mortha A, Chudnovskiy A, Hashimoto D, Bogunovic M, Spencer SP, Belkaid Y, Merad M (2014) Microbiota-dependent crosstalk between macrophages and ILC3 promotes intestinal homeostasis. Science 343(6178):1249288. https://doi.org/10.1126/science.1249288

Ojetti V, Lauritano EC, Barbaro F, Migneco A, Ainora ME, Fontana L, Gabrielli M, Gasbarrini A (2009) Rifaximin pharmacology and clinical implications. Expert Opin Drug Metab Toxicol 5(6):675–682. https://doi.org/10.1517/17425250902973695

Peteranderl C, Herold S, Schmoldt C (2016) Human influenza virus infections. Semin Respir Crit Care Med 37(4):487–500. https://doi.org/10.1055/s-0036-1584801

Sonnenberg GF, Fouser LA, Artis D (2011a) Border patrol: regulation of immunity, inflammation and tissue homeostasis at barrier surfaces by IL-22. Nat Immunol 12(5):383–390. https://doi.org/10.1038/ni.2025

Sonnenberg GF, Monticelli LA, Elloso MM, Fouser LA, Artis D (2011b) CD4(+) lymphoid tissue-inducer cells promote innate immunity in the gut. Immunity 34(1):122–134. https://doi.org/10.1016/j.immuni.2010.12.009

Swaim CD, Canadeo LA, Monte KJ, Khanna S, Lenschow DJ, Huibregtse JM (2020) Modulation of extracellular isg15 signaling by pathogens and viral effector proteins. Cell Rep 31(11):107772. https://doi.org/10.1016/j.celrep.2020.107772

Uribe-Herranz M, Bittinger K, Rafail S, Guedan S, Pierini S, Tanes C, Ganetsky A, Morgan MA, Gill S, Tanyi JL, Bushman FD, June CH, Facciabene A (2018) Gut microbiota modulates adoptive cell therapy via CD8α dendritic cells and IL-12. JCI insight 3(4). https://doi.org/10.1172/jci.insight.94952

Venkatesh M, Mukherjee S, Wang H, Li H, Sun K, Benechet AP, Qiu Z, Maher L, Redinbo MR, Phillips RS, Fleet JC, Kortagere S, Mukherjee P, Fasano A, Le Ven J, Nicholson JK, Dumas ME, Khanna KM, Mani S (2014) Symbiotic bacterial metabolites regulate gastrointestinal barrier function via the xenobiotic sensor PXR and Toll-like receptor 4. Immunity 41(2):296–310. https://doi.org/10.1016/j.immuni.2014.06.014

Waheed AA, Freed EO (2007) Influenza virus not cRAFTy enough to dodge viperin. Cell Host Microbe 2(2):71–72. https://doi.org/10.1016/j.chom.2007.07.005

Wlodarska M, Luo C, Kolde R, d'Hennezel E, Annand JW, Heim CE, Krastel P, Schmitt EK, Omar AS, Creasey EA, Garner AL, Mohammadi S, O'Connell DJ, Abubucker S, Arthur TD, Franzosa EA, Huttenhower C, Murphy LO, Haiser HJ, Vlamakis H, Porter JA, Xavier RJ (2017) Indoleacrylic acid produced by commensal

peptostreptococcus species suppresses inflammation. Cell Host Microbe 22(1):25-37.e6. https://doi.org/10.1016/j.chom.2017.06.007

Zhang D, Li S, Wang N, Tan HY, Zhang Z, Feng Y (2020) The cross-talk between gut microbiota and lungs in common lung diseases. Front Microbiol 11:301. https://doi.org/10.3389/fmicb.2020.00301

Zhang J, Zhu S, Ma N, Johnston LJ, Wu C, Ma X (2021) Metabolites of microbiota response to tryptophan and intestinal mucosal immunity: a therapeutic target to control intestinal inflammation. Med Res Rev 41(2):1061–1088. https://doi.org/10.1002/med.21752